Measuring Winds from Space to Reduce the Uncertainty in the Southern Ocean Carbon Fluxes: Science Requirements and Proposed Mission

Joellen L. Russell[1], David G. Long[2], Paul S. Chang[3], Madeline Cowell[4], Enrique Curchitser[5], Michael S. Dinniman[6], Charles Fellows[1], Paul J. Goodman[1], Eileen E. Hofmann[6], Zorana Jelenak[3], John Klinck[6], John Krasting[7], Nicole Lovenduski[8], Marcus Lofverstrom[1], Matthew Mazloff[9], Shelley Petroy[4], Anjani Polit[1], Ernesto Rodriguez[10], Oscar Schofield[5], Ad Stoffelen[11], Ronald J. Stouffer[1], Rik Wanninkhof[12], Carl Weimer[4], and Xubin Zeng[1]

Affiliations: 1. University of Arizona; 2. Brigham Young University; 3. NOAA/NESDIS/StAR; 4. Ball Aerospace; 5. Rutgers; 6. Old Dominion University; 7. NOAA/GFDL; 8. University of Colorado-Boulder; 9. Scripps Institution of Oceanography, UCSD; 10. Jet Propulsion Laboratory, California Institute of Technology; 11. KNMI; 12. NOAA/AOML

Keywords: Observing System Design, Surface Vector Winds, Scatterometer, Southern Ocean, Air-Sea Carbon Flux

Key points:

1) The current wind observing system samples Southern Ocean storms infrequently and is unlikely to directly observe the highest winds and variability

2) Southern Ocean winds are critical to the global air-sea exchange of carbon and heat

3) Adding a carefully targeted scatterometer to the observing constellation will reduce the uncertainty in the global carbon budget by focusing on the SO where the largest fraction of the air-sea exchange happens and where the current uncertainties are largest.

Plain Language Summary

The Southern Ocean is the windiest place in the world, with frequent intense storms. The winds in these storms drive large fluxes of carbon and heat between the ocean and the atmosphere. Unfortunately, these fluxes can’t be observed directly from space; we rely on wind measurements and climate reanalyses to determine them, Our space-based observing network, however, only captures winds over the Southern Ocean twice per day at best, so our estimates of the SO winds and air-sea fluxes are uncertain and about 50% of the global uncertainty in air-sea carbon exchange is associated with the Southern Ocean. We show that higher winds are consistent with reduced uptake of atmospheric carbon by the Southern Ocean. We describe our

observing system design experiment to determine the best additional scatterometer to add to the wind-observing constellation to capture more of the high winds and reduce the uncertainty in the Southern Ocean carbon budget

Abstract

Strong winds in Southern Ocean storms drive air-sea carbon and heat fluxes. These fluxes are integral to the global climate system and wind speeds that drive them are increasing. The current scatterometer constellation measuring vector winds remotely undersamples these storms and the higher winds within them, leading to potentially large biases in Southern Ocean wind reanalyses and the carbon and heat fluxes that derive from them. This observing system design study addresses these issues in two ways. First, we describe an addition to the scatterometer constellation, called Southern Ocean Storms – Zephyr, to increase the frequency of independent observations, better constraining high winds. Second, we show that potential reanalysis wind biases over the Southern Ocean lead to uncertainty over the sign of the net winter carbon flux. More frequent independent observations per day will capture these higher winds and reduce the uncertainty in estimates of the global carbon and heat budgets.

1) Introduction

The Southern Ocean is the windiest ocean basin in the world; storms play an important role in mass and heat transport and precipitation (Wei & Qin, 2016) and drive air-sea fluxes of carbon and heat, which scale non-linearly with wind speed. These strong winds, coupled with the unique geography and upper ocean processes around Antarctica, forge a connection where carbon dioxide (and heat) are readily exchanged between the atmosphere, the oceanic mixed layer and the deep ocean (Russell et al. 2006).

The World Meteorological Organization (WMO) recognizes the need for global wind sampling every 6 hours (4 x per day); preferably every 3 hours for ocean and climate applications (Bourassa et al. 2019; Stoffelen et al. 2019). This is not achieved by the existing scatterometer constellation; undersampling is acute in the Southern Ocean (SO, hereafter, Hell et al., 2020) where fast-moving storms drive an increase in carbon exchange (Matear & Lenton, 2008). Storms are frequent but inadequately sampled (only 1-2 times per day at any location), limiting independent assessment of model-based wind reanalyses. Belmonte

Rivas and Stoffelen (2019) show large SO reanalysis biases in mean and eddy flow; additional uncertainty is associated with reduced precision and accuracy of high wind speeds (Stofflen et al. 2020), and the lack of coincident rain determination (Xu & Stoffelen, 2020). Uncertainties at high wind speeds and short storm durations (Wentz et al. 2017, Chang et al. 2009, Hell et al. 2020) suggest that the current satellite-based wind observations are insufficient. Given the small spatial scales of the SO storms and their fluctuating intensities, it is likely that current satellite wind speed observations are biased low, especially in winter.

Scatterometer, radiometer, and altimeter observations of SO winds, ocean wave height, and ocean power over the last decade indicate that all are increasing (Young et al. 2011, 2017; Young & Ribal, 2019; Reguero et al. 2019). Wei and Qin (2016) note increasing SO storms during each season, although the increase was only statistically significant in summer. Verhoef et al. (2017) show increasing global winds in reanalyses but decreasing winds in collocated QuikSCAT data. Stronger winds bring more carbon-rich deep water to the surface; this decreases uptake and increases outgassing by changing the air-sea gradient, as observed by autonomous biogeochemical floats in the SO (Gray et al. 2018).

Several studies report significant uncertainties and potential biases in wind reanalysis products over the SO, especially in the highest winds (Marseille et al., 2017; Risien & Chelton, 2008; Ardhuin et al. 2011; Chawla et al. 2013, Verezemskaya et al. 2017). Sampe and Xie (2007) found that >5% of QuikSCAT winds (Spencer et al. 2000) exceeded 20 m/s over large areas south of 40°S during winter (June-August, JJA). Comparable calculations from the ERA5 reanalysis (5th reanalysis from the ECMWF; Hersbach et al. 2020) for 2018-2019 find that <1% of winter wind speeds exceed the 20 m/s threshold. Tetzner et al. (2019) found that ERA-Interim (Dee et al. 2011) and ERA5 reanalyses (Hersbach et al. 2020) underestimated monthly-mean winds over the Antarctic Peninsula by >1 m/s and partly attribute this to higher-frequency observations by the meteorological stations. Verezemskaya et al. (2017) compared QuikSCAT wind speeds in SO mesocyclones during winter (June-September; Ricciardulli & Wentz, 2015) to four different reanalysis products (ERA-Interim, Dee et al. 2011; NCEP CFSR, Saha et al. 2010; JRA55, Kobayashi et al. 2015; MERRA2, Bosilovich et al. 2016), showing that mean wind speed was underestimated in each by 1-7 m/s and the 75th percentile was underestimated by 5-10 m/s. A significant underrepresentation in the higher winds will impact the trend.

Air-sea fluxes of CO_2 and heat are not directly observable from space; we rely on bulk formulae, experiments and simulations to determine these quantities. Current estimates of the ocean's role in the global carbon budget indicate that >50% of the anthropogenic uptake of carbon from the atmosphere by the global ocean (1.4 PgC/yr in the SO of the 2.6 PgC/yr global) and 50% of the uncertainty (±0.3 PgC/yr) in air-sea CO_2 exchange occurs in the SO (Friedlingstein et al. 2020). Uncertainties in the

SO winds contribute to significant uncertainties in the global and regional carbon budgets; this uncertainty hampers prediction and challenges our carbon emission reduction projections to stabilize global atmospheric CO_2 levels.

Current estimates of the net global carbon flux (Friedlingstein et al. 2020; Iida et al. 2015; Landschutzer et al. 2016; Takahashi et al. 2014, Wanninkhof et al. 2013) rely on a method based on the observed net invasion of bomb-^{14}C to scale the gas exchange rate equation, assuming *a priori* that gas exchange scales to the square of the winds (Sweeney et al. 2007). This process depends on spatial and temporal resolution of the "observed" wind speeds (Naegler et al. 2006). Sweeney et al. (2007) note that, "no single (scaling) value can be applied for all wind products"; other parameterizations based on isotopic evidence have been proposed (e.g. Krakauer et al. 2006). Wanninkhof and Triñanes, 2017 found that a different gas exchange parameterization (Wanninkhof et al. 2009) with increased exchange above 14 m/s and below 5 m/s (relative to the standard square of wind speed) adequately represents the net invasion of bomb-^{14}C. Alternative approaches to carbon flux parameterization using high resolution surface roughness estimates (e.g. Frew et al. 2007) have not been explored in the SO. A coherent observing system with detailed calibration and validation will allow a more precise estimate of the gas exchange rate and therefore the carbon flux in the SO.

To assess the effects of missing high winds and/or increasing winds over the SO, we take advantage of a unique and powerful tool, the Biogeochemical SO State Estimate (**BSOSE**, Verdy & Mazloff, 2017). The state estimate is constrained with physical and biogeochemical observations while maintaining closed budgets and obeying dynamical and thermodynamic balances. The ocean state estimate solves for the model initial and **boundary conditions** (i.e. surface heat fluxes, freshwater and carbon) that minimize the weighted least squares sum of model-observation misfits.

When we compare net carbon flux that occurs under high winds (>10 m/s in ERA5 reanalysis) to total flux in the daily solutions from BSOSE for 2013-2018 (forced with ERA5 hourly winds), we find that >60% of the carbon flux happens under winds greater than 10 m/s, although the fraction of the SO (south of 30°S) under these high wind speeds is ~35% of the total area (Supp. Fig. S1). **We show that the air-sea carbon fluxes and upwelling consistent with stronger winds (imposed as part of an idealized experiment) indicate that the SO will change from a net carbon sink into a net carbon source during austral winter**. This change is consistent with findings of strong outgassing between the polar front and sea ice edge based on the biogeochemical float array (Gray et al. 2018). Bronselaer et al. 2020 showed that the float observations noted by Gray et al. 2018 are not reproducible without imposing stronger winds.

As proposed, SOS-Zephyr addresses key Decadal Survey questions (NASEM 2018): How can we reduce the uncertainty in the carbon cycle feedback (carbon budget), by up to a factor of 2? And how large are variations in the global carbon cycle? SOS-Zephyr reduces uncertainty in the global carbon budget by focusing on the SO where a large fraction of the air-sea carbon exchange takes place and where the uncertainties are largest; the two biggest sources of uncertainty are: 1) "Are we (now) capturing the surface vector wind field sufficiently with our observing constellation?", and 2) is our uncertainty about the vector wind field concealing a trend? All indicators point to surface winds strengthening over the SO; SOS-Zephyr's contribution to the wind field refines our uncertainty estimates of the vector wind field and the statistics of the number, size and strength of SO Storms and indicates the presence or absence of significant trend.

The second source of uncertainty is that while wind speed determines the gas exchange rate, vector wind fields determine upwelling and mixed layer depth and therefore air-sea carbon gradient. Quantifying time-varying air-sea carbon flux in the SO ***requires*** numerical simulations to quantify underlying the ocean circulation; these simulations of biogeochemistry and air-sea carbon flux in the SO vary widely. Accordingly, SOS-Zephyr proposes a scatterometer mission to capture vector winds rather than a radiometer which can only determine wind speeds.

Reducing uncertainty in SO wind speed and variability improves estimates of air-sea CO_2 exchange in this critical region. More frequent, finely-resolved measurements allow us to better quantify the SO's role in the global carbon cycle and the climate system; enhancing our ability to predict the evolution of the carbon system over the near term.

This modeling study, where faster winds are assimilated into BSOSE, indicate that stronger winds lead to significantly increased carbon outgassing along the seasonal sea ice zone in winter and enhanced outgassing during most seasons at most latitudes, likely due to increased upwelling. Heat fluxes were enhanced by stronger winds but did not change sign. We conduct an observing system simulation experiment (OSSE) within the state estimation to illustrate how adding a satellite to the existing constellation reveals a change in magnitude and potentially the sign of present-day SO air-sea CO_2 flux estimates. The study is as follows: Section 2 describes the current scatterometer constellation, the tools we use to assess performance, and the Biogeochemical SO State Estimate; Section 3 evaluates orbital and performance specifications of the scatterometer constellation, without and with the proposed SOS-Zephyr mission. Section 4 describes our experiment in BSOSE, where surface wind speeds are increased by 20% and compares the seasonal carbon and heat fluxes in the two simulations; and Section 5 presents our conclusions.

2) Data and Methods

We first assess how often per day and at what spatial resolution the existing scatterometer constellation measures SO winds. We determine the orbital and sampling details needed for an additional satellite, to reduce the uncertainty in the net air-sea exchange of CO_2 over the SO by >30% to ±0.2 PgC/yr or less.

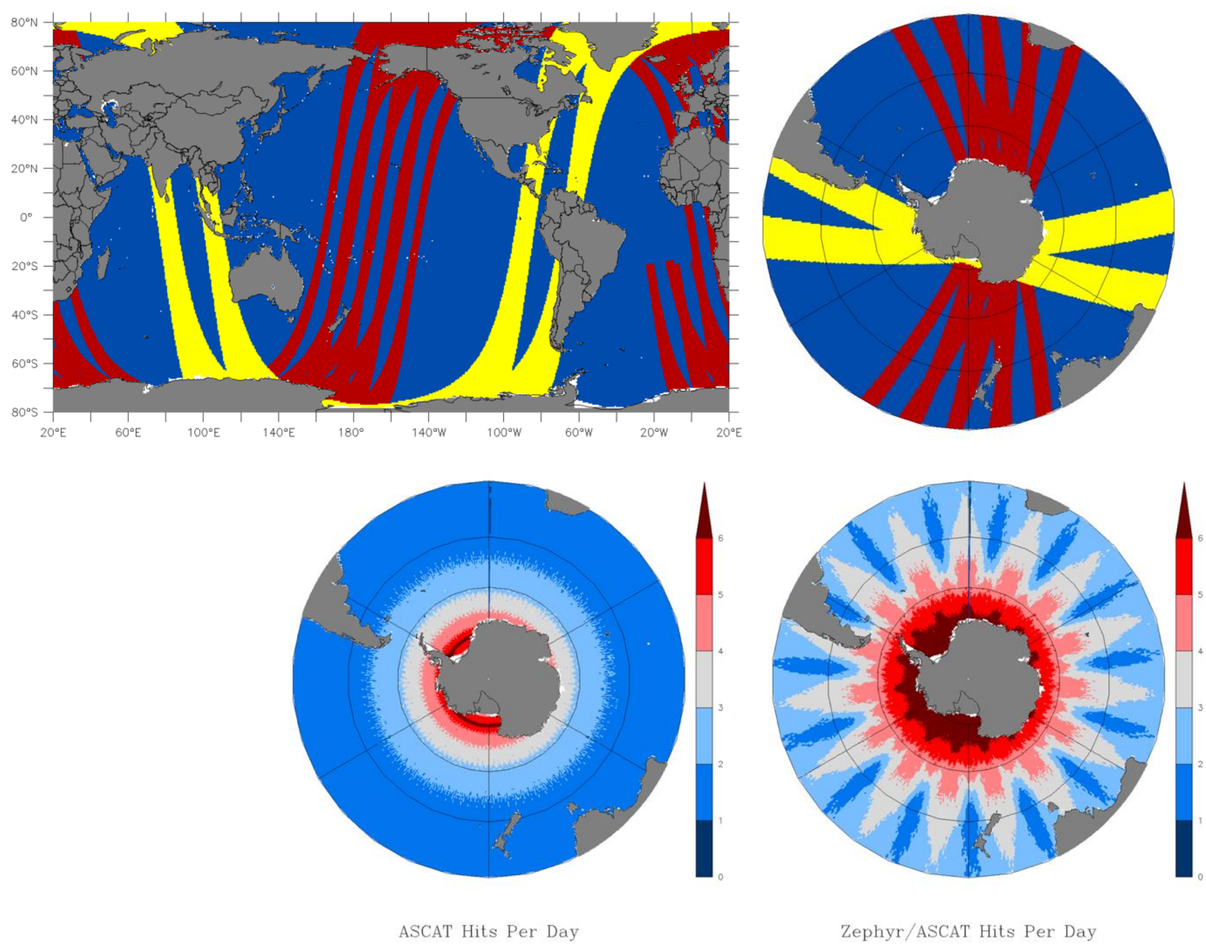

Figure 1: (A) *Locations of ground swaths during a "typical" period (3-6am GMT) for ASCAT-2 and ASCAT-3 (red) and SOS-Zephyr (yellow) with a ΔRAAN of approximately 90° and ΔLTAN of about 6 hours.* (B) *Polar plot of the same data; (C) Number of "independent" observations (defined as observations not in the same hour) per day for the constellation of ASCAT-2 and ASCAT-3; and (D) independent observations for proposed constellation (ASCAT plus SOS-Zephyr) where most locations over the Southern Ocean will be revisited 3 to 5 times per day – a 2x to 3x improvement providing the necessary temporal/spatial coverage to capture storms.*

2.1 Satellite-borne Scatterometers (ASCAT-1, ASCAT-2 & ASCAT-3)

The operational scatterometers constellation consists of three European-launched satellite missions: ASCAT-1 (Metop-A, until 2022), ASCAT-2 (Metop-B) and ASCAT-3 (Metop-C). There are three additional scatterometers currently on orbit: OSCAT2 (SCAT-SAT1; Indian Space Research Organisation, ISRO) and HY-2B/C and CFOSAT launched by China. OSCAT2 largely duplicates the ASCAT coverage (Bhowmick et al., 2019). The HY-2B satellite is in a sun-synchronous 6am/6pm orbit, while CFOSAT is a sun-synchronous 7am/7pm orbit. The temporal separation between the ASCATs and the ISRO and Chinese missions is insufficient for proper temporal sampling; they are not included in our analysis. ASCAT-2 and ASCAT-3 will still be on orbit when SOS-Zephyr is launched (2027-2028); with no knowledge of additional scatterometers in that time frame , we limit our analysis to ASCATs 2 and 3 and SOS-Zephyr.

Figure 1A and 1B show ground swaths from the ASCATs during a 3-hour period (3-6 am GMT on Day 1). During each hour, ~9% of the SO is directly observed by the ASCAT satellites and ~6.4% of the total carbon flux is "seen" directly. Figure 1C shows the daily satellite revisit cadence; for the ASCATs, only locations south of ~70°S have 4 unique visits per day, but areas north of ~53°S have 2 or fewer visits per day (12-hour return time at best). Adding ScatSat or ASCAT-3 does not change the twice-daily clustering of overpasses.

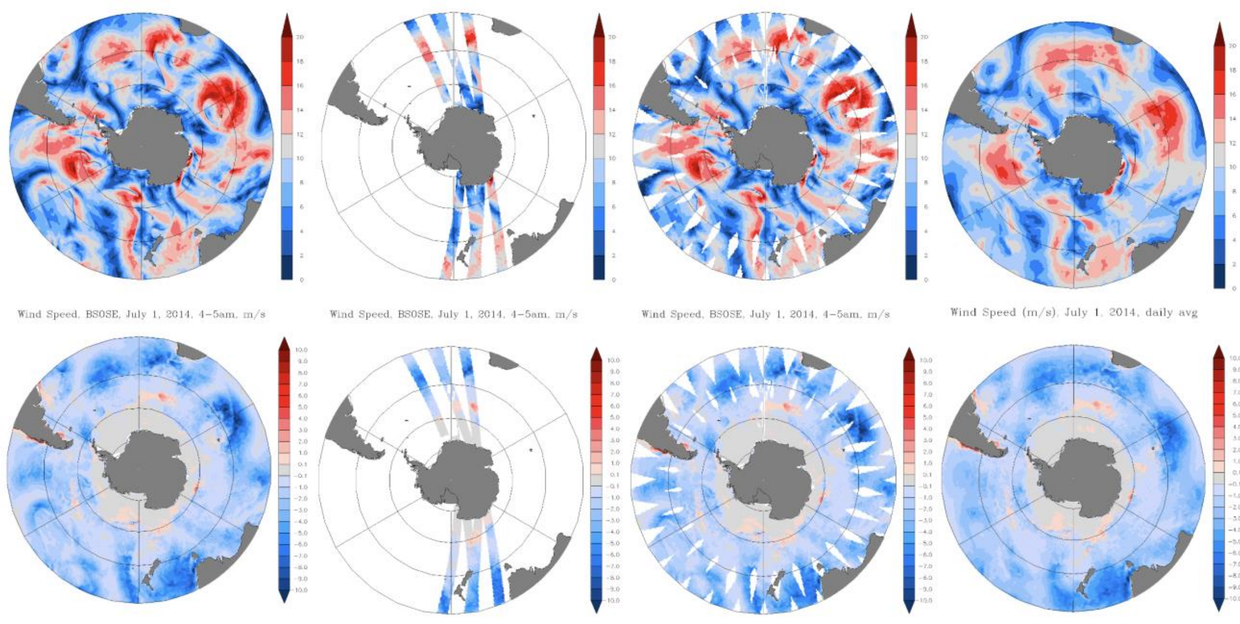

Figure 2: *(Top row, A) Wind speed (m/s) for the BSOSE solution (2013-2018) for July 1, 2014, at 4-5am (from ERA5 hourly data); (B) wind speed "seen" at 4-5am by the ASCAT-only constellation (~9% of the area); (C) wind speed "seen" by all visits of the ASCAT constellation during the day (24 hours) applied to the same wind field (~85% of the area); (D) daily average wind speed from ERA5 for July 1, 2014. (Bottom row, E) Carbon flux (mol/m^2/yr) consistent with the above winds from BSOSE at the same day/time; (F) flux "seen" by ASCAT constellation during the hour; (G) flux "seen" by all visits of the ASCAT constellation during the day (24 hours) applied to the same flux field; (H) daily average of the carbon flux from BSOSE.*

We determined where and when the constellation of satellites (ASCAT-2, ASCAT-3) observe the ocean over the course of 7 days (168 hours). We projected these observations onto hourly and daily grids of ¼°, ½° and 1° spacing, creating a series of 168 hourly "coverage maps" indicating whether a location was observed at least once by the constellation during that hour or not. We will refer to these coverage maps as "masks" because they hide the results of the model that are *unseen* by the satellites. Our results were insensitive to mask resolution; the rest of this study describes results using the ½° hourly masks. Daily masks were calculated from hourly masks (Figure 2C, 2G). We note that applying these "daily" masks to *individual hours* is more representative than applying them to the *daily average* of any particular field.

2.2 Biogeochemical SO State Estimate

The Biogeochemical SO State Estimate (BSOSE, Verdy & Mazloff, 2017) at 1/6° horizontal grid (~18km), January 2013 to December 2018, is used (http://sose.ucsd.edu/BSOSE6_iter133_solution.html). BSOSE assimilates observations from shipboard sensors, profiling floats, satellites and reanalyses (wind speeds, SST, SSS, biogeochemical data, etc.) into a numerical model, producing a state estimate for the SO. In BSOSE, the MIT general circulation model (MITgcm) is fully coupled to a Biogeochemistry with Light, Iron, Nutrients, and Gases (BLING) model (Galbraith et al. 2015). Please refer to Verdy and Mazloff (2017) for additional details.

The BSOSE solution assimilates ERA5 hourly wind speed data, so we are able to assess the ocean state consistent with any wind regime. To gauge the effects of either a low bias in the reanalysis winds and/or increasing wind speeds on the ocean (e.g. the mixed-layer depth, the surface temperature, the air-sea fluxes of carbon and heat, etc.), we ran a *perturbation* experiment where BSOSE winds are increased by 20%. This approach is similar to the idealized perturbation experiments recently published by Bronselaer et al. 2018, 2020 in which a fixed zonal wind forcing anomaly was applied to the SO surface to assess the effect of possible biases in wind stress and latitudinal position. We chose a 20% increase to envelope the effects of the possible missing winds. This experiment addresses two specific points: how do surface fluxes over the SO change in response to stronger winds, and how often must we sample the SO winds to capture either the missing winds or the trend. All other parameters for the 2013-2018 simulation were held constant from the control experiment. Increasing the winds has two direct effects on the ocean; mixed layers deepen, exposing a larger volume of water to the atmosphere, and air-sea fluxes that depend on wind speed will be greater. Either or both could alter the air-sea exchange.

3) Adding SOS-Zephyr to the Constellation

SOS-Zephyr will be a sun synchronous, conical scan, single swath instrument similar to SeaWinds on QuikSCAT (Spencer et al., 2000). Having a wider swath with overlap at lower latitudes was one of the big advantages of QuikSCAT over the ASCAT design: QuikSCAT visited 93% of the global ocean each day while the ASCAT constellation only observes 77% each day (Verspeek & Stoffelen, 2009). Many orbital details proposed for SOS-Zephyr are found in the Supplemental Methods section; the essential parameters are the swath-width of 1225km and the RAAN/LTAN of ~152° and ~3:30/15:30 respectively. The size and timing of SOS-Zephyr's ground track decreases the average revisit to less than 6 hours south of 65°S (Fig 1D, 4 per day at most longitudes) and less than 8 hours south of about 50°S (3 per day). The relative swath positions of SOS-Zephyr in our optimal orbit (Fig 1A & 1B) show excellent separation from the ASCAT swaths. Including the SOS-Zephyr coverage in the constellation increased the area observed from 9% per hour with ASCAT alone to more than 14% per hour. Fast transient changes will be better tracked by adding SOS-Zephyr; inclusion into the constellation increases the fraction of integrated carbon flux retrieved from 6.4% with ASCAT-only to 11.2% per hour (75% increase).

To quantify the net improvement per day by the augmented constellation, the daily mask of all locations visited that day by each constellation was applied to both the hourly retrievals and the daily sum of the hourly fluxes. The fraction of net flux captured by each constellation was similar in both methods; the differences between ASCAT and ASCAT+SOS-Zephyr are clear, with increases of daily capture at 96%, compared to 75% for carbon and 86% for heat for ASCAT-only.

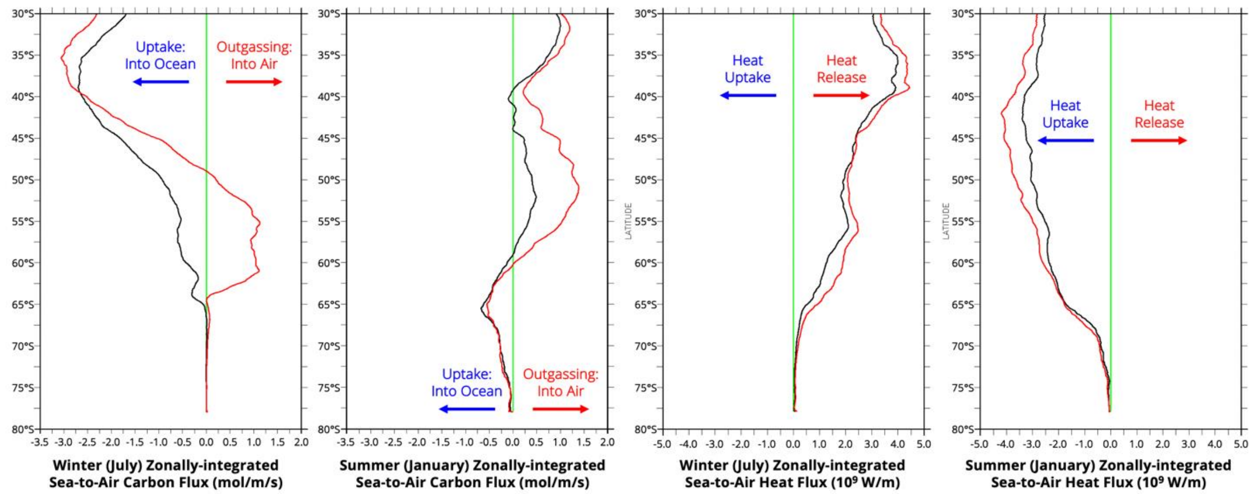

Figure 3: Comparison of carbon fluxes and heat fluxes consistent with standard ERA5 wind speeds and with 20% higher wind speeds. Carbon Fluxes (zonally-integrated) during (A) July 2014 for BSOSE-ERA5x1.0 (black), BSOSE-ERA5x1.2 (red), and (B) January 2014 for BSOSE-ERA5x1.0 (black), and BSOSE-ERA5x1.2 (red); and Heat Fluxes (zonally-integrated) for (C) July 2014 and (D) January 2014 with the same color convention. Positive (negative) values are out of (into) the ocean. Note that carbon fluxes in January of the ERAx1.0 run (panel B, black line) are generally out of the ocean except at 40°S and south of 58°S, while in the ERAx1.2 run (red line), these fluxes are more strongly out of the ocean (degassing) between 60°S and 40°S, mirroring the strong outgassing seen between 62°S and 50°S during July (A, red line) under increased winds compared to the uptake at these latitudes in July under standard winds (A, black line).

4) The Experiment: A State Estimate with Stronger Wind Speeds

To assess potential benefits of adding SOS-Zephyr to our scatterometer constellation, we pose two questions: 1) "If reanalysis winds are biased low, how would this affect the carbon and heat fluxes?" and 2) "Would adding an additional satellite capture more of these higher winds?".

Figure 3 shows zonally-integrated carbon fluxes (A,B) and total heat fluxes (C,D) for July (A,C) and January (B,D) under standard ERA5 winds (black) and stronger winds (red) in response to increasing the wind speeds. In the SO, south of about 50°S, the vertical carbon gradient in winter is strong; increased stirring brings more carbon-enriched deep water to the surface in a region of divergence where it can escape to the atmosphere. Enhanced mixing of deep carbon changes the sign of the air-sea gradient and turns the region south of 50°S from a net sink (Fig 3A, black line) taking up of 0.024 PgC for the month to a net source (red line) releasing 0.044 PgC for the month – a change of 0.067 PgC. Increased gas exchange in uptake regions at lower latitudes increase the net uptake there, but stronger divergence in the latitudes of Drake Passage (63°S-55°S) under higher winds ventilates older, deeper carbon-rich water, and turns the SO from a strong net sink taking up 0.175 PgC into a weaker net sink, only taking up 0.096 PgC. Outgassing is this region in winter near the ice edge has been documented by biogeochemically-sensored floats (Gray et al. 2018). Carbon fluxes in January are not as uniform; there is uptake at the highest latitudes adjacent to the continent, but most of the region is outgassing except along the northern edge of the Antarctic Circumpolar Current. Increasing winds turn the summer SO, south of 30°S, from a weak outgassing region with a net release of 0.020 PgC over the month into a strong outgassing region releasing 0.074 PgC. The average monthly change implies an annual change of ~0.84 PgC/yr less uptake, representing a 33% decrease in the total uptake by global ocean (2.5 PgC, and an additional atmospheric increase of ~0.4 ppm per year) or about 60% of the annual US emissions (1.4 PgC/yr in 2018, Friedlingstein et al. 2019).

This experiment illustrates that carbon fluxes respond differently to increasing winds than do heat fluxes. Heat fluxes (both in and out) are enhanced by stronger winds, while stronger winds release more carbon out of the ocean throughout the year.

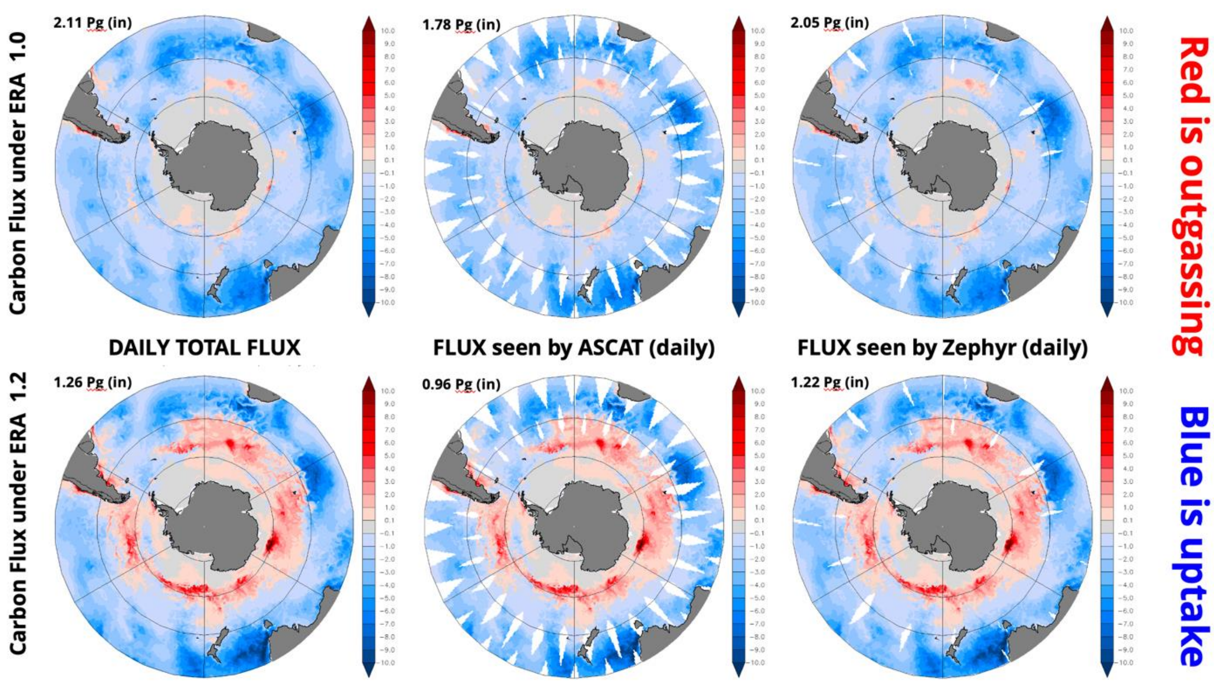

Figure 4 (Top row, A,B,C) Simulated carbon fluxes on July 1, 2014 from BSOSE-ERA5x1.0; (Bottom row, D,E,F) Simulated carbon fluxes from BSOSE-ERA5x1.2. In each panel, red (positive) is out of the ocean while blue (negative) is into the ocean. The left column (A,D) shows the total from BSOSE; the middle column (B,E) shows what is captured by the ASCAT constellation; and the right

column (C,F) shows what is captured by the addition of SOS-Zephyr. The total fluxes (PgC/yr) are indicated in the upper left corner of each panel.

4a) Carbon Flux captured by the Satellite Constellation

We next look at the differences between carbon and heat fluxes captured. On an hourly basis, ASCAT sees ~9% of the area and 6.4% of the carbon flux, while ASCAT+SOS-Zephyr sees ~14% of the area and 11.2% of the carbon. Over the course of each 24-hour interval, the ASCAT constellation visits ~88% of the SO (south of 30°S) while adding SOS-Zephyr increases that area to 97%. This increase has significant repercussions for the total fluxes of carbon and heat observed.

Figure 4 shows total surface fluxes of carbon from BSOSE assimilations for July 1, 2014. The hourly output from BSOSE was averaged over the entire day; the mask for each constellation includes locations that were visited at least once during the day. Most of the carbon flux is into the ocean except for the highest latitudes near the ice edge and the coastal regions of South America. The net carbon flux for the month is uptake of ~0.17 PgC, equivalent to ~2.1 PgC/yr. The daily average for the ASCAT-constellation represents 81% of the total flux (1.7 Pg/yr, less than the relative area covered) whereas the addition of SOS-Zephyr increases the net flux captured to 96% (2.0 Pg/yr). As can be seen, the gaps in the coverage by the ASCAT-only constellation coincide with the larger uptake fluxes, biasing the total toward the low end.

Monteiro et al (2015) support the importance of temporal resolution, noting that pCO_2 observations less than two days apart are required to reduce the annual uncertainty of the SO carbon flux below 10%. They conclude that "the synoptic period and the spatial scale of the wind stress, particularly the magnitude and phasing of storm events, make a significant contribution to reducing the uncertainty of the flux." Trindade et al. (2020) show that reanalysis differences with scatterometers can be reduced by 20% by subtracting local biases that are constant over 5 days, indicating that these biases are associated with the local ocean state rather than with the local weather. Local ocean states vary on the ocean eddy scale of a few km; we believe that the higher spatial resolution of SOS-Zephyr reduces this aspect of our uncertainty (Lindsley et al. 2016).

5) Discussion

SO winds are the strongest on average globally, but are distinctly spatially and temporally heterogeneous due to the presence of long-lasting, fast-moving storms. These winds stir the surface ocean, driving strong carbon and heat fluxes between atmosphere and ocean, especially in winter. Significant shortcomings and assumptions associated with determining the air-sea carbon fluxes over the SO persist. 1) Our current wind observing system samples these storms infrequently (once or twice per day), and is unlikely to directly observe the highest winds and variability. 2) Uncertainty in precision and accuracy of existing scatterometers are large at the highest wind speeds. 3) Climate reanalyses underestimate the mean winds by 1-7 m/s and the 75^{th} percentile by 5-10 m/s compared to scatterometer data (Vezeremskaya et al. 2017). It is these reanalysis winds that determine the SO and global carbon fluxes and budgets. 4) Determination of the wind-dependent air-sea gas exchange parameterization relies on these uncertain winds to determine the global formulation. And 5) coupled climate models consistently simulate wind speeds over the SO that are weaker and more equatorward than observed, which has a large impact on the simulated fluxes (Russell et al. 2006; Bracegirdle et al. 2013; Russell et al. 2018; Beadling et al. 2020).

By paying careful attention to the orbital parameters, this design OSSE addresses most of the above issues. 1) SOS-Zephyr increases temporal resolution to 3-6 observations per day, south of 45°S. 2) Increased spatial resolution using new processing algorithms increases precision and accuracy at the highest wind speeds and provides data close to coasts and sea ice edges, and coincident radiometer observations reduce the confounding effects of coincident rain. And 3) new wind observations and new attention to the gas exchange parameterization will refine this critical component of our carbon budget estimates. The “best” estimate of the global carbon budget (Friedlingstein et al. 2020) indicates that more than half of the net air-sea carbon flux occurs in the SO and half of the global uncertainty in the air-sea carbon flux is in the SO.

An additional, targeted scatterometer achieves our main goal of reducing the uncertainty in the global carbon budget by focusing on the SO where the largest fraction of the air-sea exchange happens and where the current uncertainties are largest. If successful, SOS-Zephyr will become a pathfinder for additional instruments that could provide a trove of new data, closing many of the holes in our understanding and quantification of the carbon and heat budgets due to weathered ocean-scale air-sea interaction.

Acknowledgments

This work was sponsored in part by NSF’s Southern Ocean Carbon and Climate Observations and Modeling (SOCCOM) Project under the NSF Awards PLR-1425989 and OPP-1936222, with additional support from NOAA and NASA. Logistical support for this project in the Antarctic was provided by the U.S. National Science Foundation through the U.S. Antarctic Program. We acknowledge the use of the Ferret program from NOAA’s Pacific Marine Environmental Laboratory for analysis and graphics (http://ferret.pmel.noaa.gov/Ferret/). We also thank the Thomas R. Brown foundation at the University of Arizona for supporting JLR.

Data availability statement.

The B-SOSE Iteration 133 output used in this analysis is available at Scripps Institution of Oceanography: http://sose.ucsd.edu/BSOSE6_iter133_solution.html.

References

Ardhuin, F., Hanafin, J., Quilfen, Y., Chapron, B., Queffeulou, P., Obrebski, M., et al. (2011). Calibration of the IOWAGA global wave hindcast (1991–2011) using ECMWF and CFSR winds. In *Proc. 12th International Workshop of Wave Hindcasting and Forecasting*, Hawaii. Joint Technical Commission for Oceanography and Marine Meteorology Technical Report No. 67, Kohala Coast, Hawaii.

Beadling, R.L., Russell, J.L., Stouffer, R.J., Mazloff, M., Talley, L.D., Goodman, P.J., et al. (2020). Representation of Southern Ocean properties across Coupled Model Intercomparison Project generations: CMIP3 to CMIP6, *J. Climate*, **33(15),** 6555-6581. https://doi.org/10.1175/JCLI-D-19-0970.1

Belmonte Rivas, M. & Stoffelen, A. (2019). Characterizing ERA-Interim and ERA5 surface wind biases using ASCAT. *Ocean Science*, **15**, 831–852. https://doi.org/10.5194/os-15-831-2019

Bhowmick, S.A., Cotton, J., Fore, A., Kumar, R., Payan, C., Rodriguez, E., et al. (2019). An assessment of the performance of ISRO's SCATSAT-1 Scatterometer. *Current Science*, **117**, 959. doi: 10.18520/cs/v117/i6/959-972.

Bosilovich, M.G., Lucchesi, R. & Suarez, M. (2016). MERRA-2: File Specification. GMAO Office Note No. 9 (Version 1.1), 73 pp. [Available at http://gmao.gsfc.nasa.gov/pubs/office_notes.]

Bourassa, M.A., Meissner, T., Cerovecki, I., Chang, P.S., Dong, X., Chiara, G.D., et al. (2019). Remotely Sensed Winds and Wind Stresses for Marine Forecasting and Ocean Modeling. *Frontiers in Marine Science*, **6**, 443. https://doi.org/10.3389/fmars.2019.00443

Bracegirdle, T.J., Shuckburgh, E., Sallee, J.-B., Wang, Z., Meijers, A.J.S., Bruneau, N., et al. (2013). Assessment of surface winds over the Atlantic, Indian, and Pacific Ocean sectors of the Southern Ocean in CMIP5 models: historical bias, forcing response, and state dependence, *J. Geophysical Research-Atmosphere*, **118**, 547–562, doi:10.1002/jgrd.50153.

Bronselaer, B., Winton, M., Griffies, S.M., Hurlin, W.J., Rodgers, K.B. , Sergienko, O.V. et al. (2018). Change in future climate due to freshwater from Antarctic ice melt, *Nature*, **564**, 53-58. https://doi.org/10.1038/s41586-018-0712-z

Bronselaer, B., Russell, J.L.,Winton, M. Williams, N.L., Key, R.M., Dunne, J.P. et al. (2020). Importance of wind and meltwater for observed chemical and physical changes in the Southern Ocean, *Nature Geosciences*, **13**, 35-42. https://doi.org/10.1038/s41561-019-0502-8

Chang, P.S., Jelenak, Z., Sienkiewicz, J., Knabb, R., & Brennan, M. (2009). Operational Utilization and Impact of Satellite Remotely-Sensed Ocean Surface Vector Winds in the Marine Warning and Forecasting Environment. *Oceanography Magazine*, **22,** 194–207. https://doi.org/10.5670/oceanog.2009.49

Chawla, A., Spindler, D.M. & Tolman, H.L. (2013). Validation of a thirty-year wave hindcast using the Climate Forecast System Reanalysis winds. *Ocean Modelling*, **70**, 189-206. doi: 10.1016/j.ocemod.2012.07.005

Dee, D.P., Uppala, S.M., Simmons, A.J., Berrisford, P., Poli, P., Kobayashi, S., et al. (2011). The ERA-Interim reanalysis: configuration and performance of the data assimilation system. *Quarterly Journal of the Royal Meteorological Society,* **137**, 553–597. https://doi.org/10.1002/qj.828

Frew, N.M., Glover, D.M., Bock, E.J. & McCue, S.J. (2007). A new approach to estimation of global air-sea gas transfer velocity fields using dual-frequency altimeter backscatter, *J. Geophysical Research*, **112**, C11003, doi:10.1029/2006JC003819

Friedlingstein, P., Jones, M.W., O'Sullivan, M., Andrew, R.M., Hauck, J., Peters, G., et al. (2019). Global Carbon Budget 2019, *Earth System Science Data*, **11**, 1783–1838. https://doi.org/10.5194/essd-11-1783-2019

Friedlingstein, P., O'Sullivan, M., Jones, M.W., Andrew, R.M., Hauck, J., Olsen, A. et al. (2020). Global Carbon Budget 2020. *Earth System Science Data*, **12**, 3269–3340. https://doi.org/10.5194/essd-12-3269-2020

Galbraith, E.D., Dunne, J.P., Gnanadesikan, A., Slater, R.D., Sarmiento, J.L., Dufour, C.O. et al. (2015), Complex functionality with minimal computation: Promise and pitfalls of reduced-tracer ocean biogeochemistry models, *J. Advances in Modeling Earth Systems*, **7**, 2012–2028, doi:10.1002/2015MS000463.

Gray, A.R., Johnson, K.S., Bushinsky, S.M., Riser, S.C., Russell, J.L., Talley, L.D., et al. (2018). Autonomous Biogeochemical Floats Detect Significant Carbon Dioxide Outgassing in the High-Latitude Southern Ocean. *Geophysical Research Letters*, **45**. https://doi.org/10.1029/2018GL078013

Hell, M.C., Gille, S.T., Cornuelle, B.D., Miller, A.J., Bromirski, P.D., & Crawford, A.D. (2020). Estimating Southern Ocean Storm Positions With Seismic Observations. *Journal of Geophysical Research: Oceans*, **125(4).** https://doi.org/10.1029/2019jc015898

Hersbach, H, Bell, B, Berrisford, P, Hirahara, S., Horányi, A., Muñoz-Sabater, J., et al. (2020). The ERA5 global reanalysis. *Quarterly Journal of the Royal Meteorolical Society*, **146**, 1999– 2049. https://doi.org/10.1002/qj.3803

IIda, Y., Kojima, A., Takatani, Y., Nakano, T., Sugimoto, H., Midorikawa, T., & Ishii, M. (2015). Trends in p$CO_2$and sea-air CO_2 flux over the global open oceans for the last two decades. *Journal of Oceanography*, **71**, 637–661. https://doi.org/10.1007/s10872-015-0306-4

Kobayashi, S., Ota, Y., Harada, Y., Ebita, A., Moriya, M., Onoda, H., et al. (2015), The JRA-55 reanalysis: General specifications and basic characteristics, *Journal of the Meteorological Society of Japan. Series II*, **93(1),** 5–48. https://doi.org/10.2151/jmsj.2015-001

Krakauer, N.Y., Randerson, J.T., Primeau, F.W., Gruber, N., & Menemenlis, D. (2006). Carbon isotope evidence for the latitudinal distribution and wind speed dependence of the air-sea gas transfer velocity. *Tellus B*, **58**, 390-417, doi: 10.1111/j.1600-0889.2006.00223.x.

Landschützer, P., Gruber, N. & Bakker, D.C.E. (2016). Decadal variations and trends of the global ocean carbon sink, *Global Biogeochemical Cycles*, 30, 1396– 1417. doi:10.1002/2015GB005359.

Lindsley, R.D., Blodgett, J.R. & Long, D.G. (2016). Analysis and Validation of High-Resolution Wind from ASCAT, *IEEE Transactions on Geoscience and Remote Sensing*, **54(10)**, 5699-5711. doi:10.1109/TGRS.2016.2570245

Marseille, G.J., Stoffelen, A., van den Brink, H. & Stepek, A. (2017). WISC Intermediate Bias Derivation and Uncertainty Assessment, Copernicus Climate Change Service (C3S) Wind Information Service (WISC) report, KNMI, de Bilt, the Netherlands, REF.: (C3S_441_Lot3_WISC_SC2-D3.3-CGI-RP-17-0071), https://wisc.climate.copernicus.eu/wisc/documents/shared/C3S_WISC_Intermediate_Bias_Derivation_and_Uncertainty_Assessment_v1-0.pdf

Matear, R. J., & Lenton, A. (2008). Impact of Historical Climate Change on the Southern Ocean Carbon Cycle, *Journal of Climate*, **21(22),** 5820-5834. https://journals.ametsoc.org/view/journals/clim/21/22/2008jcli2194.1.xml

Monteiro, P.M.S., Gregor, L., Lévy, M., Maenner, S., Sabine, C.L. & Swart, S. (2015). Intraseasonal variability linked to sampling alias in air-sea CO_2 fluxes in the Southern Ocean, *Geophysical Research Letters*, **42**, 8507– 8514. doi:10.1002/2015GL066009.

Naegler T., Ciais P., Rodgers K. & Levin I. (2006). Excess radiocarbon constraints on air-sea gas exchange and the uptake of CO2 by the oceans. *Geophysical Research Letters,* **33**: L11802, doi:10.1029/2005GL025408.

National Academies of Sciences, Engineering, and Medicine. 2018. *Thriving on Our Changing Planet: A Decadal Strategy for Earth Observation from Space.* Washington, DC: The National Academies Press. doi: https://doi.org/10.17226/24938

Reguero, B.G., Losada, I.J. & Méndez, F.J. (2019). A recent increase in global wave power as a consequence of oceanic warming. *Nature Communications,* **10,** 205. https://doi.org/10.1038/s41467-018-08066-0

Ricciardulli, L., & Wentz, F.J. (2015). A Scatterometer Geophysical Model Function for Climate- Quality Winds: QuikSCAT Ku-2011. *J. Atmospheric and Oceanic Technology*, **32**, 1829-1846. DOI: 10.1175/JTECH-D-15-0008.1

Risien, C.M., & Chelton, D.B. (2008). A Global Climatology of Surface Wind and Wind Stress Fields from Eight Years of QuikSCAT Scatterometer Data. J. Phys. Oceanogr., 38, 2379-2413. https://doi.org/10.1175/2008JPO3881.1

Russell, J.L., Dixon, K.W., Gnanadesikan, A., Stouffer, R.J. & Toggweiler, J.R. (2006). The Southern Hemisphere Westerlies in a Warming World: Propping Open the Door to the Deep Ocean. *J. Climate*, **19(24)**, 6382-6390. https://doi.org/10.1175/JCLI3984.1

Russell, J.L., Kamenkovich, I., Bitz, C., Ferrari, R., Gille, S.T., Goodman, P.J. et al. (2018). Metrics for the Evaluation of the Southern Ocean in Coupled Climate and Earth System Models, *J. Geophysical Research – Oceans*, **123,** 3120-3143. https://doi.org/10.1002/2017JC013461

Saha, S., Moorthi, S., Pan, H., Wu, X., Wang, J., Nadiga, S., Tripp, P., et al. (2010). The NCEP Climate Forecast System Reanalysis, *Bulletin of the American Meteorological Society*, *91*(8), 1015-1058. https://doi.org/10.1175/2010BAMS3001.1

Sampe, T., & Xie, S. (2007). Mapping High Sea Winds from Space: A Global Climatology, *Bulletin of the American Meteorological Society*, **88(12**), 1965-1978. https://journals.ametsoc.org/view/journals/bams/88/12/bams-88-12-1965.xml

Spencer, M.W., Wu, C., & Long, D.G. (2000). Improved resolution backscatter measurements with the SeaWinds pencil-beam scatterometer. *IEEE Transactions on Geoscience and Remote Sensing*, **38(1)**, 89–104. https://doi.org/10.1109/36.823904

Stoffelen A., Kumar R., Zou J., Karaev V., Chang P.S. & Rodriguez E. (2019). Ocean Surface Vector Wind Observations. In: Barale V., Gade M. (eds) *Remote Sensing of the Asian Seas*. Springer, Cham. https://doi.org/10.1007/978-3-319-94067-0_24

Stoffelen, A., Mouche, A., Polverari, F., van Zadelhoff, G.-J., Sapp, J., Portabella, M., et al. (2020). C-band High and Extreme-Force Speeds (CHEFS), EUMETSAT project report, EUMETSAT ITT 16/166, https://www.eumetsat.int/CHEFS; https://www.eumetsat.int/media/45432

Sweeney, C., Gloor, E., Jacobson, A.R., Key, R.M., McKinley, G., Sarmiento, J.L., & Wanninkhof, R. (2007), Constraining global air-sea gas exchange for CO_2 with recent bomb ^{14}C measurements, *Global Biogeochemical Cycles*, **21**, GB2015, doi:10.1029/2006GB002784

Takahashi, T., Sutherland, S.C., Chipman, D.W., Goddard, J.G., Ho, C., Newberger, T. et al. (2014). Climatological distributions of pH, pCO2, total CO2, alkalinity, and CaCO3 saturation in the global surface ocean, and temporal changes at selected locations. *Marine Chemistry*, **164**, 95-125, https://doi.org/10.1016/j.marchem.2014.06.004

Trindade, A., Portabella, M., Stoffelen, A., Lin W. & Verhoef, A. (2020). ERAstar: A High-Resolution Ocean Forcing Product, *IEEE Transactions on Geoscience and Remote Sensing*, **58(2)**, 1337-1347, doi: 10.1109/TGRS.2019.2946019

Verdy, A. & Mazloff, M.R. (2017). A data assimilating model for estimating Southern Ocean biogeochemistry, *J. Geophysical Research-Oceans*, **122**, 6968– 6988, doi:10.1002/2016JC012650

Verezemskaya, P., Tilinina, N., Gulev, S., Renfrew, I.A. & Lazzara, M. (2017). Southern Ocean mesocyclones and polar lows from manually tracked satellite mosaics, *Geophysical Research Letters*, **44**, 7985–7993, doi:10.1002/2017GL074053

Verhoef, A., Vogelzang, J., Verspeek, J. & Stoffelen, A. (2017). Long-Term Scatterometer Wind Climate Data Records, *IEEE Journal of Selected Topics in Applied Earth Observations and Remote Sensing*, **10(5)**, 2186-2194. doi: 10.1109/JSTARS.2016.2615873

Verspeek, J., & Stoffelen, A. (2009). ASCAT tandem coverage, EUMETSAT Ocean and Sea Ice (OSI) Satellite Application Facility (SAF) report, v0.8, https://cdn.knmi.nl/system/data_center_publications/files/000/068/323/original/ascat_tandem_coverage.pdf?1495621136

Wanninkhof, R., Asher, W.E., Ho, D.T., Sweeney, C.S. & McGillis, W.R. (2009). Advances in quantifying air-sea gas exchange and environmental forcing. *Annual Reviews of Marine Science*, **1**, 213–244, doi:10.1146/annurev.marine.010908.163742.

Wanninkhof, R., Park, G.-H., Takahashi, T., Sweeney, C., Feely, R., Nojiri, Y., et al. (2013). Global ocean carbon uptake: magnitude, variability and trends. *Biogeosciences*, **10**, 1983–2000. https://doi.org/10.5194/bg-10-1983-2013

Wanninkhof, R. & Triñanes, J. (2017). The impact of changing wind speeds on gas transfer and its effect on global air-sea CO2 fluxes. *Global Biogeochemical Cycles*, **31**, 961–974, doi:10.1002/ 2016GB005592

Wei, L., & Qin, T. (2016). Characteristics of cyclone climatology and variability in the Southern Ocean. *Acta Oceanologica Sinica*, **35**, 59–67, doi: 10.1007/s13131-016-0913-y

Wentz, F., Ricciardulli, L., Rodriguez, E. Stiles, B., Bourassa, M., Long, D. et al. (2017). Evaluating and Extending the Ocean Wind Climate Data Record. *IEEE Journal of Selected Topics in Applied Earth Observations and Remote Sensing*. **99**, 2165–2185. doi: 10.1109/JSTARS.2016.2643641

Xu, X. & Stoffelen, A. (2020). Improved Rain Screening for Ku-Band Wind Scatterometry, *IEEE Transactions on Geoscience and Remote Sensing*, **58:4**, 2494-2503. doi: 10.1109/TGRS.2019.2951726

Young, I.R., & Ribal, A. (2019). Multiplatform evaluation of global trends in wind speed and wave height. *Science*, **364(6440)**, eaav9527. https://doi.org/10.1126/science.aav9527

Young, I.R., Sanina, E., & Babanin, A.V. (2017). Calibration and Cross Validation of a Global Wind and Wave Database of Altimeter, Radiometer, and Scatterometer Measurements. *Journal of Atmospheric and Oceanic Technology*, **34(6)**, 1285–1306. https://doi.org/10.1175/jtech-d-16-0145.1

Young, I.R., Zieger, S., & Babanin, A.V. (2011). Global Trends in Wind Speed and Wave Height. *Science*, **332(6028)**, 451–455. https://doi.org/10.1126/science.1197219